

Nucleation of Oxygen Precipitates in Czochralski Single-Crystal Silicon Quenched from High Temperature

Atsushi Ikari*¹Hiroyo Haga*¹Osamu Yoda*²Akira Uedono*³Yusuke Ujihira*⁴

Abstract:

The nucleation of oxygen precipitates as Czochralski process-grown single-crystal silicon (Cz-Si) is quenched from a high temperature of 1,390°C after solution treatment was studied to clarify factors responsible for defective nucleation in the Cz-Si crystal on cooling during pulling. It was found that the nucleation of oxygen precipitates depends on cooling conditions from the high temperature, that the density of nuclei increases with increasing quenching start temperature, and that the nucleation is suppressed by slow cooling. The formation, transformation, and annihilation behaviors of irradiation defects during electron beam irradiation (at 3 MeV and $1 \times 10^{18} e^-/cm^2$) and subsequent isochronal annealing were investigated by infrared absorption and positron annihilation techniques. The nuclei for oxygen precipitation were found to be oxygen clusters.

1. Purpose of Study

Silicon crystals, which are used as substrates for ultralarge-scale integration (ULSI) for memory and other microelectronic devices, are probably the most crystallographically perfect of materials that can now be industrially produced. Silicon crystals are claimed to be free from dislocations and defects, but contain defects when observed at an atomic level. As microelectronic devices have dramatically increased in circuit density and decreased in circuit size in recent years, atomic-level defects, which were rather ignored in the past, have come to be highlighted¹⁾. These defects have not yet been identified, but are believed to deteriorate the properties of devices, such as lowering the breakdown voltage of the gate oxide, and to nucleate the defects that occur in the silicon crystal in the heat treatment step of the device

fabrication process.

It has become necessary to control and suppress the occurrence of atomic-level defects in the silicon crystal. The occurrence of such defects changes with the growth conditions and cooling conditions (thermal history) of the silicon crystal. In the silicon crystal grown by the Czochralski process (Cz-Si crystal), oxygen contained in the Cz-Si crystal is considered to interact in a complex manner on cooling, nucleating oxygen precipitates and oxidation-induced stacking faults (OSF).

This study focused attention on oxygen precipitation and investigated its nucleation to clarify the formation mechanism of defective nucleation in the Cz-Si crystal on the atomic level.

All the wafers used for ULSI devices are made from Cz-Si crystals. This is because the oxygen contained in the Cz-Si crystal increases the mechanical strength of the wafer and prevents the wafer warpage that is harmful for device fabrication (lithography, in particular). Lately, a device contamination prevention technique (intrinsic gettering²⁾) has come to be employed where appropriate oxygen precipitates are created within the wafer

*1 Technical Development Bureau

*2 Japan Atomic Energy Research Institute

*3 University of Tsukuba

*4 University of Tokyo

so as to collect and neutralize the contaminating heavy metal atoms that are introduced during the device fabrication process. If oxygen precipitates are formed on the wafer surface on which devices are built, they, of course, make the devices inoperative. Therefore, how to control the oxygen precipitation is critical for bringing out the merits of oxygen (strength gain and gettering) while suppressing its harmful effects (precipitation-caused malfunction). The precipitation of oxygen widely varies with the thermal history of the Cz-Si crystal during pulling. This is because oxygen precipitation nuclei are formed in the cooling step of the Cz-Si crystal growth process.

Many studies were carried out to clarify the substance and formation mechanisms of oxygen precipitation nuclei³⁾. Most of the past studies investigated the distribution of nuclei in Cz-Si crystals fabricated under given pulling conditions and tried to elucidate the formation mechanism of nuclei from that distribution^{4,5)}. These approaches have the advantage of feeding back the results directly to crystal fabrication conditions, but a complex entanglement of various factors makes it extremely difficult to verify the validity of nucleation models developed from such research results. The free thermal history control of actual ingots is difficult to achieve owing to the influence of the growth interface and the high heat capacity of the ingot.

To clarify the effect of thermal history on defective nucleation, the authors quenched Cz-Si crystals in a heat treating furnace from the vicinity of melting point to room temperature and investigated the formation of oxygen precipitation nuclei. The specimens were solution treated. That is, the oxygen precipitates formed during the Cz-Si crystal formation were dissolved to "reverse" the thermal history of Cz-Si crystal formation. The solubility limit of oxygen in the silicon material used in the experiment is 1,300°C⁶⁾. The oxygen precipitates are considered to be dissolved above this temperature. The specimen was heat treated at 1,390°C for 2 h, and then cooled rapidly and slowly (at 1°C/min corresponding to the cooling rate in the puller) to introduce oxygen precipitation nuclei into the specimen. The precipitation behavior of oxygen was investigated by precipitation heat treatment, and the substance of the defective nuclei introduced by the quenching operation was clarified by positron annihilation and infrared absorption techniques.

2. Analysis of Defects by Positron Annihilation Technique^{7,8)}

The positron annihilation technique, which was traditionally used with great results in the research of lattice defects in metals, has come to be applied to semiconductors as well⁹⁾ and has now become an indispensable tool for the study of defects in semiconductors.

When positrons are driven into a crystal, they are annihilated in pairs with the corresponding electrons in the crystal and emit gamma rays. Since positrons have a positive charge, they are subject to the Coulomb repulsion from the atomic nucleus. They are high in abundance in interstitial position in the vicinity of atoms. If there are vacancies or other defects in the crystal, positrons are high in abundance at such crystal defects, and have a high probability of being captured there. If there are about 10⁻⁵ defects relative to crystal lattice points, positrons will be absolutely annihilated at the defects. If the defects have a negative charge, the probability of positrons being captured by them

will increase further. Thus, lattice defects like vacancies can be identified by examining gamma rays emitted at the annihilation of positrons.

The pair annihilation of an electron and a positron usually emits two gamma rays. These two gamma rays are emitted in opposite directions conforming to the momentum conservation law. The momentum of the positron is practically lost before the capture of the positron by a defect. Since the electron to be annihilated in the pair retains its momentum, the gamma ray it emits deviates from a straight line by the momentum (see Fig. 1). The angular deviation caused by the momentum of the electron is observed as the gamma ray energy shift due to the Doppler effect. If the electron is a bound electron like a core electron of an atom, its momentum has a wide spread. The spread of the gamma ray energy due to the Doppler effect is thus wide.

If the electron is a conduction electron, it has a given value of momentum, and the broadening of the energy shift is small. At defects like vacancies where there are no atoms and core electrons, many positrons are annihilated in pairs with conduction electrons, and the energy shift broadening is small. At interstitial defects, conversely, the proportion of positrons being annihilated in pair with core electrons increases, and so does the energy shift broadening. The technique of measuring the energy shift broadening to obtain information on point defects is called the Doppler broadening measuring method. In the Doppler broadening measurement, the degree of energy shift broadening is indicated by a value called the S parameter. In Fig. 2, the S parameter is defined by

$$S = \text{counts in gray region} / \text{total counts} \quad \dots\dots (1)$$

The value of S decreases with increasing spectral broadening. A large value of S indicates the presence of vacancy defects, while a small value of S indicates the presence of interstitial defects.

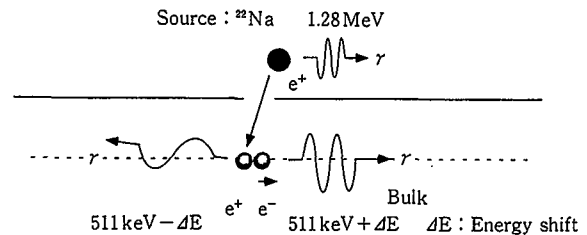


Fig. 1 Pair annihilation of electron and positron in crystal

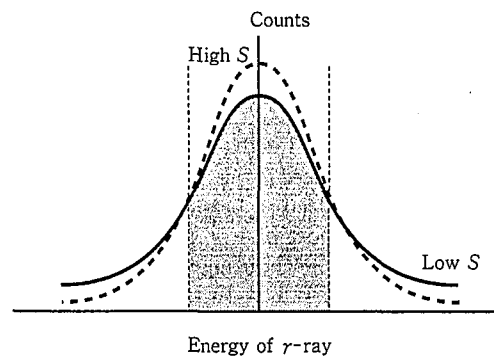


Fig. 2 Spectrum of Doppler broadening measurement and S parameter

The positron lifetime measuring method determines the time from the introduction to the annihilation of positrons. In other words, the time between the detection of the 1.28-MeV gamma ray generated when positrons are emitted by the decay of the radiation source ^{22}Na and the detection of the 511-keV gamma ray generated when the positrons are annihilated is measured. The positrons driven into the Cz-Si crystal are decelerated (turned into heat) by interaction with electrons or phonons, converted into energy at room temperature, captured by defects, and annihilated. The time required for the deceleration of positrons is short (about 10^{-12} s), and the lifetime of positrons depends on the time from their capture to annihilation, which in turn depends on the density of electrons in the defects. Vacancies are free of atoms and low in electron density, and extend the lifetime of positrons. Conversely, interstitial defects are high in electron density and shorten the lifetime of positrons. Dannefaer et al.⁹⁾ measured the lifetime of positrons in silicon crystals, and obtained the values of 216 ps for the bulk of defect-free crystals, 270 ps for monovacancies and 320 ps for divacancies.

Two or more types of lifetime, including components from the positron radiation source, are actually measured in duplication. The lifetime spectra thus obtained are deconvoluted to obtain the intensity ratio of the lifetime values or components. Using a program called POSITRONFIT¹⁰⁾, the present analysis fixed the two lifetimes of 270 ps (monovacancies) and 320 ps (divacancies), divided the lifetime data into three components (four components if the radiation source component is included), and determined the intensity of each component. The capture rate κ_i was calculated from the lifetime intensity, using a simple trapping model (reaction kinetics of positrons captured by defects and the annihilation process). κ_i is related to defect concentration C_i as given by

$$\kappa_i = \mu_i C_i \quad \dots\dots (2)$$

where μ_i is the probability of positrons being captured by the i -th defect.

3. Experimental Methods

The specimens used in the experiment were boron-doped Cz-Si crystals having a resistivity of $10 \Omega\text{-cm}$ and measuring 25 by 25 by 2 mm. The solid oxygen concentration of specimens was 1×10^{18} atoms/cm³. Specimens were solution treated in a helium atmosphere at 1,390°C for 2 h. The solution-treated specimens were cooled in helium gas and liquid nitrogen, respectively, at rates of 2,000 and 3,500°C/min. Some specimens were slowly cooled in helium gas at a rate of 1°C/min from 1,300 to 1,000°C (see Fig. 3). The quenched specimens were chemically etched on both surfaces to remove 200 μm and were polished on both surfaces to mirror finish.

The density of oxygen precipitates was measured by selective etching after annealing at 1,000°C for 23 h. To examine the precipitation nuclei introduced in the quenching step, the solution-treated specimens were electron beam irradiated at an incident energy of 3 MeV and a dose of $1 \times 10^{18}\text{e}^-/\text{cm}^2$. The specimen temperature was about 150°C during the electron beam irradiation. The electron beam-irradiated specimens were isochronally annealed for 30 min each from 100°C to 1,100°C and were examined by the positron annihilation and infrared absorption techniques.

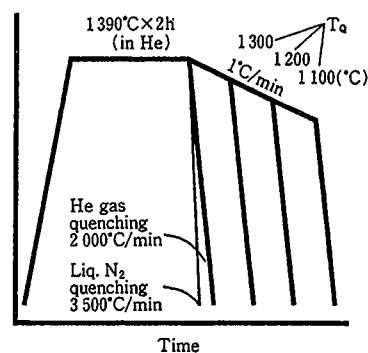


Fig. 3 Solution treatment and quenching

4. Experimental Results

4.1 Oxygen precipitation behavior of quenched specimens

Fig. 4 shows the density of oxygen precipitates in the solution-treated and quenched specimens that were heat treated in the nitrogen atmosphere at 1,000°C for 23 h for oxygen precipitation. The density of oxygen precipitates was a very high $2 \times 10^{11}/\text{cm}^3$ when the solution-treated specimens were quenched from 1,390°C. The density of oxygen precipitates does not depend on the precipitation heat treatment temperature, but is strongly influenced by the quenching start temperature T_Q and decreases with decreasing quenching start temperature T_Q . These results show that stable oxygen precipitation nuclei are introduced in the quenching step. The density of oxygen precipitation nuclei was found to provide activation energies of 4.9 and 1.9 eV in the T_Q ranges of 1,390 to 1,200°C and 1,200 to 1,000°C, respectively. The solubility limit of oxygen in the specimens is about 1,300°C⁶⁾. If oxygen is not involved in this nucleation, the density of oxygen precipitates should become constant above 1,300°C. The experimental results, however, show the density of oxygen precipitates to monotonously increase even above 1,300°C. This suggests the participation of intrinsic point defects in the formation of oxygen precipitation nuclei.

4.2 Analysis of precipitation nuclei by infrared absorption and positron annihilation techniques

Fig. 5 shows the values of S parameter for the Doppler broadening of solution-treated and quenched specimens (see Fig. 3). The higher the quenching rate and the higher the quenching start temperature T_Q , the smaller the value of S parameter. The quenching operation was found to have introduced interstitial defects. When specimens were electron beam irradiated, the value of S parameter rose on the whole because of the development

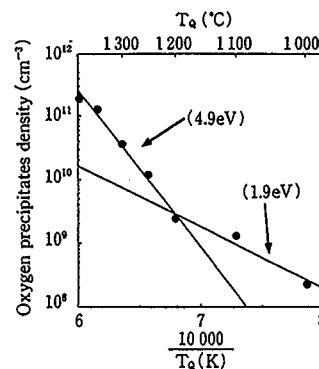


Fig. 4 Change in density of oxygen precipitates with quenching start temperature after solution treatment

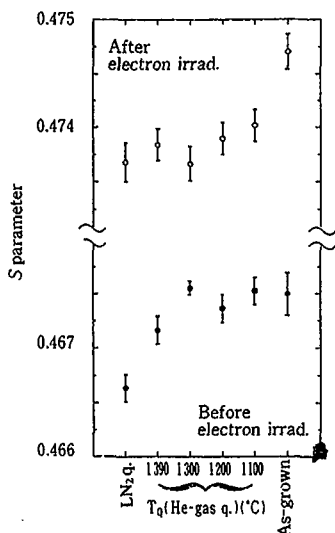


Fig. 5 Doppler broadening of solution-treated specimens

of vacancy defects by the electron beam irradiation. The tendency for the value of S parameter to decrease with increasing quenching start temperature T_Q remains unchanged after the electron beam irradiation. This indicates that the formation of irradiation defects is influenced by defects introduced by the quenching operation.

The infrared absorption spectra of specimens revealed a strong absorption band at 830 cm^{-1} . This absorption band is attributable to vacancy-oxygen complex pairs (VO)¹¹⁾ and indicates that the irradiation-induced vacancies combined with oxygen in solid solution to form the vacancy-oxygen complex pairs. The formation of VO is high in the as-grown specimens that are not quenched before the electron beam irradiation and low in those specimens quenched before the electron beam irradiation (see Fig. 6). A weak absorption band was observed at $1,014\text{ cm}^{-1}$. The intensity of this absorption band was inversely correlated with the intensity of VO.

Fig. 7 shows the relationship between the infrared absorption and isochronal annealing temperature of as-grown specimens not quenched but electron beam irradiated. The 830-cm^{-1} absorption band of VO starts to attenuate at 300°C , and at the same time, another absorption band appears at 890-cm^{-1} . The 890-cm^{-1} absorption band is attributable to monovacancy-two oxygen atom complex pairs (VO_2)¹²⁾, which are formed by the diffusion of oxygen by the reaction $\text{VO} + \text{O} \rightarrow \text{VO}_2$ ¹³⁾. At 540°C , VO_2 is annihilated by the reaction $\text{VO}_2 + \text{O} \rightarrow \text{VO}_3$. Complexes of various sizes are formed and annihilated by these reactions, and their formation and annihilation behaviors are observed by the infrared absorption technique. In particular, the absorption band at $1,014\text{ cm}^{-1}$ is stable to a maximum temperature of 900°C . The source of this absorption band is probably a vacancy-oxygen complex pair VO_n ($n > 2$) having more than two oxygen atoms combined with a vacancy. Since the oxygen precipitation occurs as soon as the absorption band disappears, the complex is considered to work as a nucleus for the oxygen precipitation.

Fig. 8 shows positron lifetime measurements for the same as-grown specimens as in Fig. 7. The value of κ_2 that indicates the concentration of defects having the lifetime of monovacancies disappears at 540°C , the temperature at which VO_2 is annihilated. This is because VO and VO_2 have roughly the same lifetime

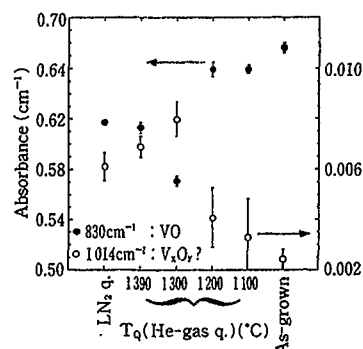


Fig. 6 Concentration of vacancy-oxygen complex pairs after electron beam irradiation

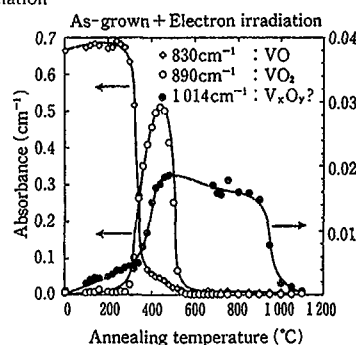


Fig. 7 Change in infrared absorption with isochronal annealing temperature for as-grown specimens

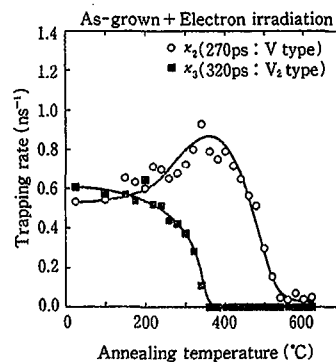


Fig. 8 Change in positron lifetime with isochronal annealing temperature for as-grown specimens

as monovacancies¹⁴⁾, and κ_2 indicates the concentration of both VO and VO_2 . The value of κ_3 indicating the concentration of divacancies (V_2) is reduced at about 350°C . V_2 is known to be diffused and annihilated at about 250°C ¹⁵⁾, but κ_3 does not disappear at 250°C , probably because V_2 combines with oxygen to form such complexes as $V_2\text{O}$ and $V_2\text{O}_2$. At about 300°C , κ_3 decreases, whereas κ_2 increases. This is because larger complexes are formed by the diffusion of oxygen, initiated at 300°C , by the reaction $V_2\text{O}_x + \text{O} \rightarrow V_2\text{O}_{x+1}$, and their lifetime is reduced to the neighborhood of 270 ps. Since oxygen is an interstitial defect, a combination of many oxygen atoms is considered to shorten the positron lifetime.

Figs. 9 and 10 respectively show the infrared absorption and positron lifetime measurements of specimens quenched in helium gas from $1,390^\circ\text{C}$ after the solution treatment. Quenched specimens differ from as-grown specimens in that a strong absorption band at $1,014\text{ cm}^{-1}$ appears from the beginning. The

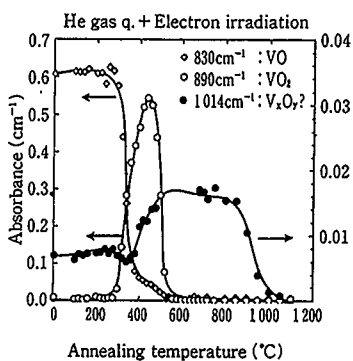


Fig. 9 Change in infrared absorption with isochronal annealing temperature for helium gas-quenched specimens

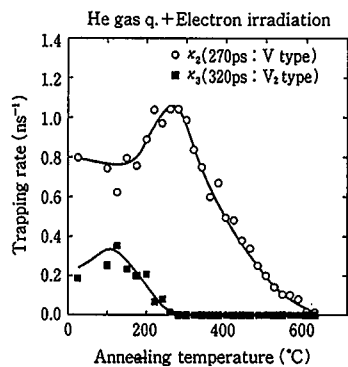


Fig. 10 Change in positron lifetime with isochronal annealing temperature for helium gas-quenched specimens

1,014-cm⁻¹ absorption band is presumably attributable to VO_n. This means that oxygen clusters (O_n) are introduced by the quenching operation. As compared with as-grown specimens, quenched specimens have x₃ decreased and x₂ increased at 250°C. Since oxygen clusters are already formed in the quenched specimens, they are thought to combine with V₂ to shorten the lifetime of V₂ as soon as V₂ begins to diffuse.

The inverse correlation between the intensities of 1,014 cm⁻¹ and 830 cm⁻¹ (VO) shown in Fig. 6 may be explained this way:

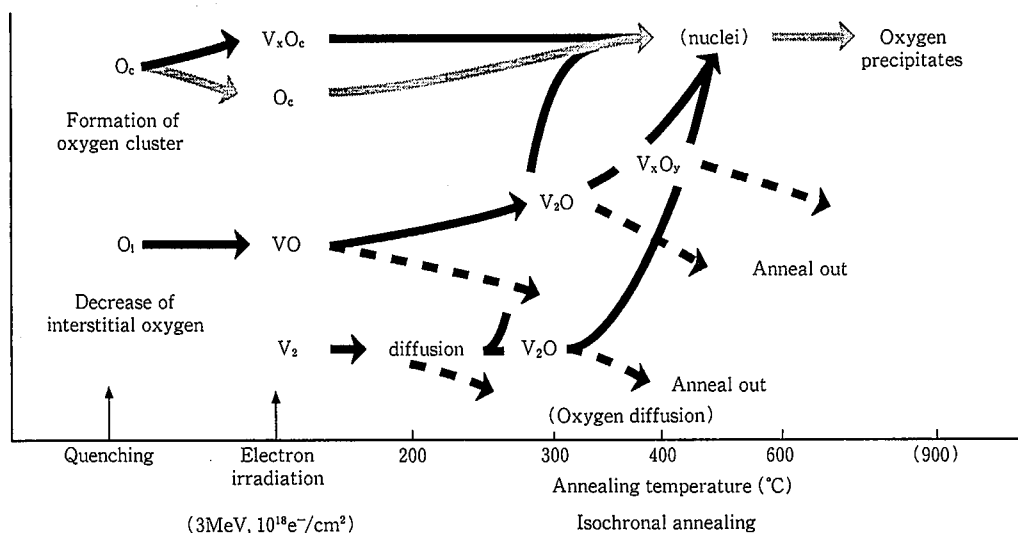


Fig. 11 Formation of oxygen clusters by quenching and formation of vacancy-oxygen complex pairs by electron beam irradiation

The oxygen clusters formed by the quenching operation reduce the concentration of isolated oxygen atoms, which in turn reduces the concentration of VO. The decrease in the value of S parameter in the quenched specimens shown in Fig. 5 may be ascribed to the fact that oxygen clusters are interstitial defects. If the oxygen clusters are attributable to quenching, the difference in the measured results between quenched specimens and as-grown specimens can be explained without difficulty.

5. Conclusions

The nucleation of oxygen precipitation in silicon crystals in the process of cooling from a high temperature was investigated. It was found that the nucleation of oxygen precipitates depends on cooling conditions. That is, rapid cooling increases the density of oxygen precipitates, while slow cooling retards the formation of oxygen precipitation nuclei. The defect formation behavior under electron beam irradiation was investigated by the infrared absorption and positron annihilation techniques. A strong absorption band was observed at 1,014 cm⁻¹ in quenched specimens. Since VO formation was small, it was evident that oxygen clusters were introduced to serve as nuclei for oxygen precipitation (see Fig. 11).

References

- 1) Tsuya, H. et al.: Oyo Buturi. 60, 752 (1991)
- 2) Tan, T.Y. et al.: Appl. Phys. Lett. 30, 175 (1977)
- 3) Lin, W.: Semiconductor Silicon 1990. Montreal, 1990, ECS, p. 569
- 4) Harada, H. et al.: Semiconductor Silicon 1986. Boston, 1986, ECS, p. 76
- 5) Shimanuki, Y. et al.: J. Electrochem. Soc. 136, 2058 (1989)
- 6) Mikkelsen, Jr. J.C.: Oxygen, Carbon, Hydrogen and Nitrogen in Crystalline Silicon. Boston, 1985, MRS, p. 19
- 7) West, R.N.: Adv. Phys. 22, 263 (1973)
- 8) Brandt, W.: Proc. Intern. School of Physics "Enrico Fermi" Course 83, Positron Solid-State Physics. Verenna, North-Holland, 1983
- 9) Dannefaer, S.: Defect Control in Semiconductor. Yokohama, 1989, IC-STDS (North-Holland), p. 1561
- 10) Kirkegaard, P. et al.: Comp. Phys. Commun. 23, 307 (1981)
- 11) Corbett, J.W. et al.: Phys. Rev. 121, 1015 (1961)
- 12) Stein, H.J.: Appl. Phys. Lett. 48, 1540 (1986)
- 13) Svensson, B.G. et al.: Phys. Rev. B34, 8709 (1986)
- 14) Dannefaer, S.: Phys. Stat. (a). 102, 481 (1987)
- 15) Chen, L.J. et al.: Phys. Rev. 152, 761 (1966)